IEEE Access
Multidisciplinary | Rapid Review | Open Access Journal

Received March 14, 2020, accepted March 27, 2020, date of publication March 31, 2020, date of current version April 14, 2020.

Digital Object Identifier 10.1109/ACCESS.2020.2984537

Energy Cost Optimization of Hybrid Renewables Based V2G Microgrid Considering Multi Objective Function by Using Artificial Bee Colony Optimization

HABIB UR RAHMAN HABIB[1,2], UMASHANKAR SUBRAMANIAM[3], (Senior Member, IEEE), ASAD WAQAR[4], BASHAR SAKEEN FARHAN[5], KOTB M. KOTB[6,7], AND SHAORONG WANG[1]

[1]School of Electrical and Electronics Engineering, Huazhong University of Science and Technology, Wuhan 430074, China
[2]Department of Electrical Engineering, Faculty of Electrical and Electronics Engineering, University of Engineering and Technology Taxila, Taxila 47050, Pakistan
[3]Renewable Energy Laboratory, College of Engineering, Prince Sultan University, Riyadh 11586, Saudi Arabia
[4]Department of Electrical Engineering, Bahria University, Islamabad 44000, Pakistan
[5]Electrical Engineering Department, Engineering College, Al-Iraqia University, Baghdad 10053, Iraq
[6]Electrical Power and Machines Engineering Department, Faculty of Engineering, Tanta University, Tanta 31512, Egypt
[7]Electric Power Department, Faculty of Engineering and Informatics, Budapest University of Technology and Economics, 1111 Budapest, Hungary

Corresponding author: Habib Ur Rahman Habib (hr_habib@hust.edu.cn)

ABSTRACT The worldwide demand for reduction of CO2 pollution, with more penetration of renewable energy sources and an increased number of electric vehicles (EVs), demonstrates the importance of economic dispatch (ED) with taking into account the reduction of CO2 emission. ED is a classical problem in which EVs impose more penetration as a dynamic load, and its impact as vehicle-to-grid (V2G) is the possible future trend with cost minimization. Based on the integration of EVs and hybrid renewable sources concerning both economic dispatch and pollution minimization, the multi-objective function is converted into a single comprehensive objective by using the judgment matrix methodology. In this paper, the investigation involves the minimization of the cost of all three objectives viz. operation cost, pollution cost, and carbon emissions with ED by incorporating V2G technology. The algorithms which include particle swarm optimization, as well as artificial bee colony, are applied under various operation and control strategies. The proposed models are verified and analyzed with different case studies. In terms of operation economics, the simulation results validate the superior performance of EVs based microgrid (MG) model in the coordinated charging and discharging mode. Further, the comparison of both algorithms shows better results with the ABC algorithm in terms of cost minimization of all objectives. ABC is better in V2G based microgrid with coordinated charging and discharging mode while its performance is significant during a large number of EVs (i.e., 700 EVs). Moreover, the load shedding scenarios are integrated which enables the MG system to operate in dual mode (i.e., seamless transition). In this paper, the main contribution involves penetration of EVs as dynamic load and its V2G impact in a coordinated or uncoordinated way, application of ABC algorithm for this particular load problem with improved results, and inclusion of short-term load shedding scenarios.

INDEX TERMS Vehicle-to-grid (V2G), electrical vehicles (EVs), particle swarm optimization (PSO), artificial bee colony (ABC), dynamic ED, operating cost (OC), pollutant treatment cost (PTC), carbon dioxide emission (CE).

NOMENCLATURE

ABBREVIATIONS

PG	Power Grid
WT	Wind Turbine
MT	Micro Gas Turbine
PV	Photovoltaic
DE	Diesel Engine
DG	Diesel Generator
FC	Fuel Cell
BSS	Battery Storage System
PSO	Particle Swarm Optimization
TP	Thermal Plants
DERs	Distributed Energy Resources

The associate editor coordinating the review of this manuscript and approving it for publication was Yanbo Chen.

RES	Renewable Energies Sources
MOED	Multi-Objective ED
ABC	Artificial Bee Colony
OC	Operation Cost
SOED	Single Objective Economic Dispatch
PTC	Pollutant Treatment Cost
LSS	Load Shedding Scenarios
CE	Carbon Dioxide Emissions
CHP	Combined Cooling Heating and Power
GA	Genetic Algorithm
IP	Interior Point
PS	Pattern Search
EP	Evolutionary Programming
EBCO	Enhanced Bee Colony Optimization
HIC	Hybrid Imperialist Competitive
GWA	Grey Wolf Algorithm
FLC	Fuzzy Logic Controller
DP	Dynamic Programming
MPC	Model Predictive Control
COM	Classical Optimization Method
ARO	Adjustable Robust Optimization
V2G	Vehicle-To-Grid
SOC	State of charge

I. INTRODUCTION

For the time being, the integration of renewable energy sources (RESs) has been significantly increased due to the global energy decline as well as the increase of environmental concerns represented in greenhouse gases (GHG emission). However, with distributed energy resources (DERs), the concept of microgrid (MG) has been exaggerated [1]. It has reshaped the power grid to fully utilize both the renewable energy sources (RESs) and the distributed energy generation (DEG).

Along with the revolution of MGs, the later penetration of electric vehicles (EVs) of clean energy sources that have almost zero pollutant emissions as compared to conventional combustion engines is considered the beginning of a new era [2]. Although the combustion engines are considered more economical, EVs cost is expected to be decreased when the improvement of the energy storage technology with declining fossil fuels will happen soon. The charging of EVs affects the main grid performance in terms of increasing peak hours, and fluctuations of the voltage and frequency [3], [4]. With the intervention of vehicle-to-grid (V2G) technology [5], the above mentioned issues will become obsolete. With the utilization of bidirectional converters, bidirectional power flow is, therefore, possible to have access to power from the utility grid and even to supply it as DERs with the use of power converters while EVs are plugged-in. However, by controlling the charging/discharging process of EVs that installed in an MG, peak load could be shifted, and therefore, a reliable and economical grid operation can be achieved [6], [7].

Economic dispatch (ED) is considered the fundamental concern for operation engineers working with any MG system. Dynamic ED transforms the MG model into discrete-time equations with small steps (i.e., in minutes which can be solved with 1 or 5 minutes steps) followed by static ED for solving each minute's intervals [8]. In this way, this strategy will work as the consecutive scheduling according to the real MG operation.

Many researchers have chosen multi-objective function with consideration of different objectives, which include operating costs along with the emission and environmental considerations with the help of various dispatch algorithms mentioned in [9], [10]. Many kinds of researches have been carried out about the ED as mentioned above problems which include minimum fuel cost, low SO2 emissions, low NOx emissions in [11]. At the same time, unified consideration of SO2 and NOx altogether was not assumed in terms of environmental pollution. In [12], GHG emission was analyzed, except CO2 emissions, as an individual objective function entity rather than combining it with pollutant emissions. NSGA-II was implemented in [11] and [13]; however, it was only possible for solving one duration of schedule, but the dynamic ED which was designed to handle the consecutive durations, was observed in [12]. The charging/discharging and demand-side phenomena for photovoltaic based grid-connected MG with EVs, transferable loads and distributed resources were examined in [14]. The operating cost (OC) is considered as objective function with four cases. While multi-objective seeker optimization was applied with fuzzy logic. The authors in [15] proposed a power routing strategy for EVs based unbalanced hybrid MG system. The objective function involves minimization of power loss and power imbalance factor along with improved system load ability as well as voltage profile. For DC MG system, fast EVs charging scheme is proposed in [2] with virtual-battery based droop control with improved bus voltage, ED and battery State of Charge (SOC).

The OC was taken as an objective function by authors in [16] and was not considered in [17], even though the V2G operation was taken in both cases. In [18], a single cost function was assumed, and the performance of different algorithms was analyzed. Carbon dioxide emission (CE) with other objective functions was considered in [19] as multi-objective functions without considering OC, CE and pollutant treatment cost (PTC). Authors considered the only grid-connected case in [20] without considering renewables penetration with V2G technology, while no optimization with cost function was carried out. A single objective function was examined in [21] and the performance of multi-optimization algorithms was investigated without considering the V2G scenario. Authors in [22], minimization of OC was recognized as a single objective function without considering OC, CE, and PTC. Model predictive control was applied in [23], [24] with consideration of OC and PTC, while the V2G scenario was out of scope. Only the V2G case without optimization cost functions was studied in [25]. A single

TABLE 1. Summary of related research on EVs.

Ref.	Study System	V2G	LSS	MOED			SOED	Tools/Algorithms
				OC	PTC	CE		
[16]	WT-PV-CHP-BSS	Yes	No	Yes	No	No	Yes	CPLEX
[17]	WT-PV-BSS	Yes	No	No	No	No	Yes	GA-IP-PS
[18]	WT-PV-BSS	No	No	No	No	No	Yes	EP-GA-PSO-BCO-EBCO
[19]	WT-PV	No	No	No	No	Yes	No	HIC-GWA
[20]	-	Yes	No	No	No	No	No	FLC
[21]	WT-PV-DG-FC-BSS	No	No	No	No	No	Yes	PSO-GA-ABC-FLC
[22]	PV-BSS	Yes	No	Yes	No	No	Yes	DP
[23]	WT-PV-MT-FC-BSS	No	No	Yes	Yes	No	No	MPC
[25]	RES-BSS	Yes	No	No	No	No	No	-
[24]	WT-PV-DE-BSS	No	No	Yes	Yes	No	No	PSO
[26]	-	Yes	No	No	No	No	Yes	COM
[27]	WT-TP-BSS	Yes	No	Yes	No	Yes	No	PSO-FLC
[28]	WT-PV-MT-DE-BSS	Yes	No	Yes	Yes	No	No	ARO
[29]	WT-PV-DE-FC-BSS	Yes	No	Yes	Yes	Yes	Yes	PSO
Present work	WT-PV-DE-FC-BSS	Yes	Yes	Yes	Yes	Yes	Yes	PSO-ABC

objective function was solved with the V2G case in [26] without keeping in view the integration of renewable energy resources as well as multi-objective cost functions (OC, PTC, CE). V2G with OC and CE in [27] was elaborated without PTC. In [28], V2G with OC and PTC was expressed without CE cost function and PV generation. V2G with OC and PTC was taken in [28] and [29] while the additional cost factor of CE was also considered in [29]. Table 1 shows a summary of relevant research that was performed on EVs in recent times. It is observed from Table 1 that almost all of the literature considered particular objectives out of all three proposed objectives mentioned in this study.

The contribution of this paper can be highlighted as follows: ED optimization considering OC, PTC, and CE using ABC algorithm, the effect of EV on ED with different charging modes and scheduling strategies, The DES consisting of PV, WT, DE, FC and Battery Storage System (BSS), the results of ABC algorithms are compared with the results of PSO algorithms.

After a comprehensive review of literature studies, it is concluded that Economic dispatch (ED) is a classical problem in which the existing approaches rarely used detailed analysis of EVs as dynamic load in both coordinated as well as un-coordinated way. At the same time, ABC is not applied to this particular type of ED problem. Furthermore, short-term load shedding scenarios are also not discussed in the literature studies during ED. Due to energy shortage and greenhouse gas (GHG) emissions globally, the new future trend involves high penetration of EVs and its application as a vehicle to grid (V2G). Therefore, more advanced algorithms like ABC are required to solve more complicated ED problems. As compared to other existing approaches, the ABC algorithm does not trap in local minima during the search of the best optimal solution. The specific attribute of the ABC algorithm is the limit cycle which is identified by a scout bee to avoid local minima. In this paper, the main contribution involves penetration of EVs as dynamic load and its V2G impact in a coordinated or uncoordinated way, application of ABC algorithm for this particular load problem with improved results, and inclusion of short-term load shedding scenarios.

II. THE LOAD MODELS OF EVS

A. SPATIAL AND TEMPORAL ATTRIBUTES

The proposed study presented the EVs system for domestic hybrid PEVs. The owner's driving preferences are considered as a spatial characteristic of EVs. The probability function with consideration of daily mileage of EVs is expressed as [30]:

$$f_s(x) = \frac{1}{x}.\frac{1}{\sigma_s\sqrt{2\pi}}\exp\left(-\frac{(\ln x-\mu_s)^2}{2\sigma_s^2}\right) \tag{1}$$

Also, the similar relationship for ending time is [30]:

$$f_t(x) = \begin{cases} \dfrac{1}{\sigma_t\sqrt{2\pi}}\exp\left(-\dfrac{(x-\mu_t)^2}{2\sigma_t^2}\right), \\ \qquad \mu_t - 12 < x < 24 \\ \dfrac{1}{\sigma_t\sqrt{2\pi}}\exp\left(-\dfrac{(x-(\mu_t-24))^2}{2\sigma_t^2}\right), \\ \qquad 0 < x < \mu_t - 12 \end{cases} \tag{2}$$

where $\mu_s = 8.920$; $\sigma_s = 3.240$; $\mu_t = 17.470$; $\sigma_t = 3.410$.

EVs data follows a normal distribution, and our data which is taken from [29], follows a normal distribution, and therefore, it is selected for this research study.

B. AUTONOMOUS MODE

The preference is the owners who can conveniently initiate EV charging, keeping in view any of the policies imposed by the government while the EV scheduling process is not active. The unidirectional power flow with the charging period is expressed as:

$$T_C = \frac{SW_{100}}{100P_C\eta_{C\_EV}} \tag{3}$$

where W_{100} shows the power utilization (kWh/100km), P_C is charging power (kW), η_{C_EV} is charging efficiency.

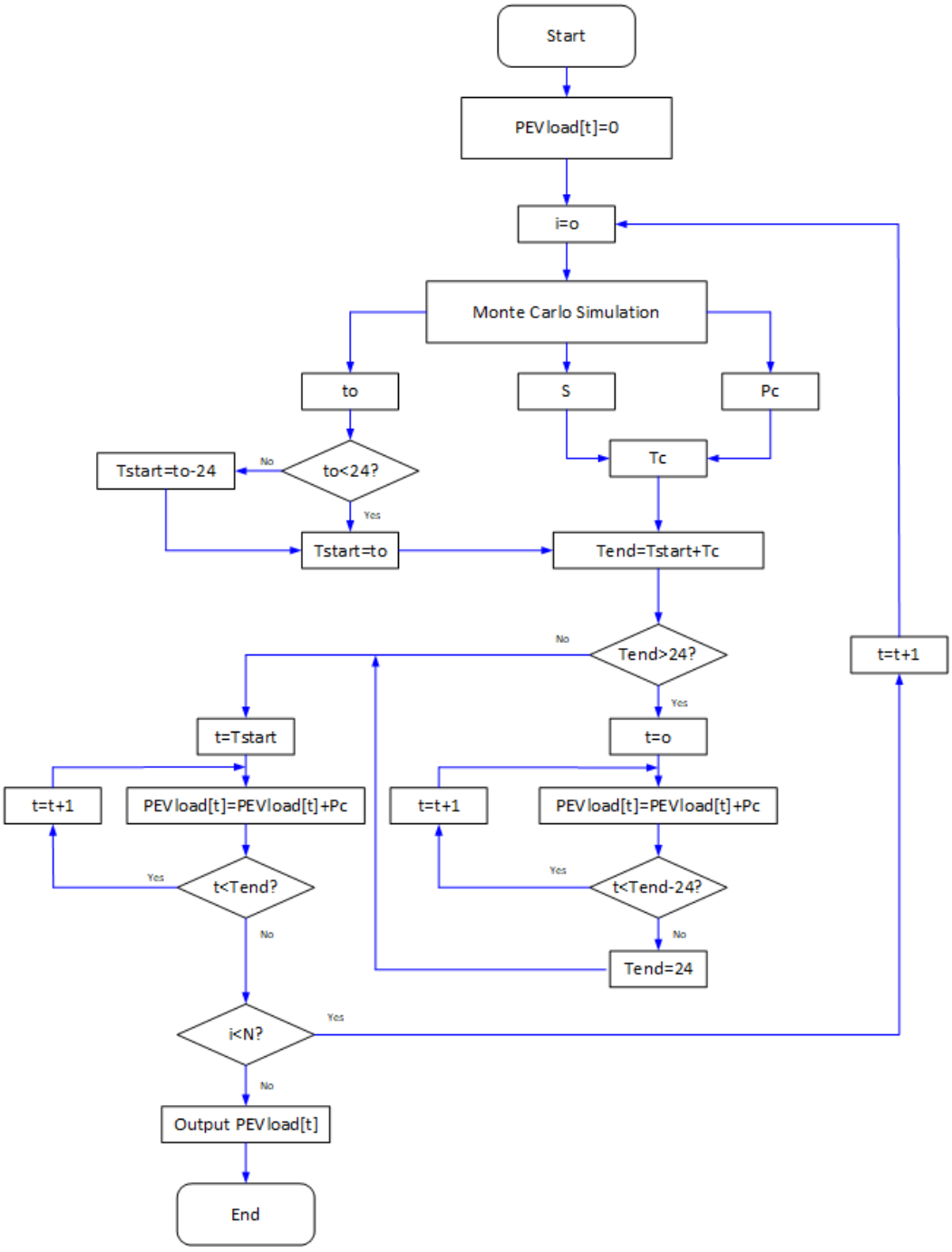

(a)

FIGURE 1. Flow diagram for computational load (a) autonomous mode.

The sum of the charging load $P_{EVload}(t)$ can be calculated by adding the values of every duration interval. As for charging periods of EVs are not dependent on one another; therefore, the daily load curve can be found with the following relationship as:

$$P_{EVload}(t) = \sum_{i=1}^{N} P_i(t) \tag{4}$$

where N is the sum of vehicles; $P_i(t)$ is the charging power; i is duration interval t (kW). Fig. 1 (a) shows the autonomous mode flowchart.

C. COORDINATED MODE

The coordinated mode (V2G) is meant to control EVs properly and centrally by keeping in view the electricity pricing policy and the behavior of the owners. Grid-connected EVs

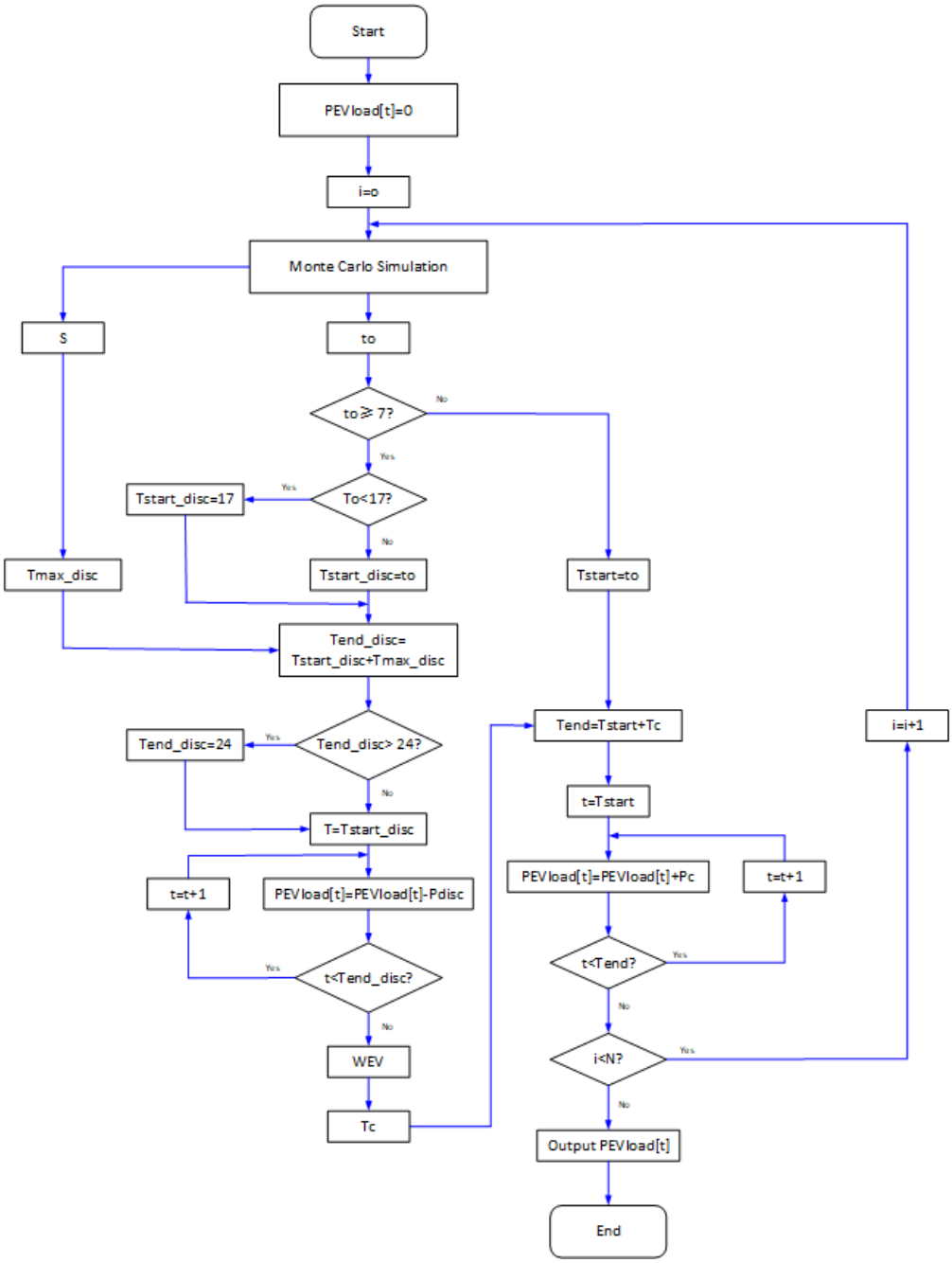

(b)

FIGURE 1. *(Continued.)* **Flow diagram for computational load (b) coordinated mode.**

which are scheduled are analyzed. The assumption is made that these EVs can be completely scheduled. EVs will be charged during off-peak load durations, while EVs will be discharged during peak load hours.

The maximum discharging duration can be calculated from the battery SOC, daily mileage, and discharging power as follows:

$$T_{\max\_disC} = \frac{(SOC_{\max} - SOC_{\min})\, C_{EV}}{P_{disC}} - \frac{SW_{100}}{100 P_{disC}} \quad (5)$$

The actual discharging time T_{disC} when EVs are discharging can be calculated as follows:

$$T_{disC} = T_{end\_disC} - T_{start\_disC} \quad (6)$$

The EV charging demand is the sum of total utilization in the everyday period, which includes daily transport utilization and discharge capacity as follows:

$$W_{EV} = P_{disC} T_{\max\_disC} - P_{disC} T_{disC} \quad (7)$$

Then expression for the charge duration is as follows:

$$T_C = \frac{W_{EV}}{P_C \eta_{C\_EV}} \tag{8}$$

Equation (4) will provide a total EV charging load. A coordinated mode flow chart is shown in Fig. 1 (b).

III. MODELING OF MULTI-OBJECTIVE COST FUNCTIONS

A. COST FUNCTIONS

The function based on multiple objectives problem with n-dimension decision variables is mathematically expressed in the following way [29]:

$$\begin{aligned} &\min F = \{f_1(x), f_2(x), \ldots, f_k(x)\} \\ &s.t. \\ &\begin{cases} g_i(x) \le 0; i = 1, 2, \ldots, q \\ h_j(x) = 0; j = 1, 2, \ldots, p \end{cases} \end{aligned} \tag{9}$$

where $x = (x_1, x_2, \ldots, x_n)$ are decision variables based on n-dimension; $f_k(x)$ is the kth objective, $g_i(x) \le 0$ and $h_j(x) = 0$ are inequality and equality constraints respectively.

ED objectives of MG which are analyzed in this paper are as follows:

1) OPERATING COST

The OC (C_1) of the MG is expressed:

$$\min C_1 = C_{Fuel} + C_{OM} + C_{DC} + MC_{GRID} + (1 - M)C_{LS} \tag{10}$$

where C_{Fuel}, C_{OM}, C_{GRID}, C_{LS}, and M are fuel cost; O&M cost; interaction cost between MG and power grid (PG); compensation cost for interruptible load; grid connection/disconnection indication respectively. M = 1 indicates MG is connected with PG, while M = 0 shows a standalone mode of the MG.

In the cost functions and formulas (10), the energy loss cost is not considered. Economic dispatch (ED) problems typically handle generation sources while distribution and transmission losses are generally out of the scope of the ED problem. We picked reference paper problems [29] and applied the ABC algorithm while no change in the problem is made.

The depreciation cost (C_{DC}) is determined [29]:

$$C_{DC} = \frac{InCost * \left[\frac{d(1+d)^l}{(1+d)^l - 1}\right]}{P_{\max} * 8760 * cf} * P_i \tag{11}$$

where $P_i, i, cf, InCost, d, l$ and $P_{\max}$ are output power; capacity factor; installation cost; interest rate (8%); DG lifetime; and DG maximum power respectively.

About the pollutant emissions types and the corresponding cost, we only considered three pollutants, namely CO2, SO2, and NOx. The emission parameters along with the corresponding weight as well as processing costs, are mentioned in Table 5.

2) POLLUTANT TREATMENT COST

The pollutant treatment cost (C_2) of the MG is:

$$\min C_2 = \sum_{i=1}^{K} \sum_{k} (C_k \gamma_{ik}) P_i + \sum_{k} (C_k \gamma_{Gridk}) P_{Grid} \tag{12}$$

where $K, k, C_k, \gamma_{ik}, \gamma_{Gridk}$, and P_{Grid} are the sum of total DGs; pollutants emissions type; treatment cost; pollutant emissions coefficient; coefficient of grid pollutant emissions; and grid output power respectively.

3) CARBON EMISSIONS COST

The carbon emission cost (C_3) can be expressed as:

$$\min C_3 = \sum_{i=1}^{K} C_{CO_2} \gamma_{iCO_2} P_i + C_{CO_2} \gamma_{GridCO_2} P_{Grid} \tag{13}$$

where $C_{CO_2}\gamma_{iCO_2}$ and γ_{GridCO_2} are the carbon treatment cost, coefficient emissions, and coefficient of grid emissions, respectively.

B. CONVERSION TO SINGLE OBJECTIVE FUNCTION

The judgment matrix methodology (JMM) expressed in [31] finds the weight of the objective, which is also a reflection of the situation and the owner's priority. The proposed study applied JMM to find the weight coefficients for every objective and finally combine in a single objective, as follows [29]:

$$C = \omega_1 C_1 + \omega_2 C_2 + \omega_3 C_3 \tag{14}$$

where $\omega_1, \omega_2, \omega_3$ are the weight coefficients for each objective. The main idea of the judgment matrix method is to find a judgment matrix that which objective has more priority. Based on the analytic hierarchy process expressed in [32], the criteria are shown in Table 2:

TABLE 2. The criteria for the judgment matrix.

Judgment number	Explanation
1	Priority is the same.
3	One objective has a moderate priority than others.
5	One objective has the highest priority than others.
Reciprocals	Both objectives have reciprocal values.

Every objective (OC, PTC, CE) is graded in three categories. Table 2 shows the judgment numbers with priorities, and the matrix can be expressed:

$$J = \begin{bmatrix} 1 & 3 & 5 \\ \frac{1}{3} & 1 & 3 \\ \frac{1}{5} & \frac{1}{3} & 1 \end{bmatrix} \tag{15}$$

After calculation, weight coefficients are found as $\omega_1 = 0.6370$, $\omega_2 = 0.2583$, $\omega_3 = 0.1047$.

According to the judgment number in table 2, there are many matrices which can be expressed, but the authors choose the formulas (15) due to the following reasons:

- Because the multi-objective problem can be represented in two ways, namely single objective, and Pareto-front.

- As the single objective representation of the multi-objective problem is straightforward. Therefore, a judgment number matrix is used.
- In multi-objective optimization, the objectives to be improved are conflict. For the convenience of the description, assuming all the objectives are to be minimized.
- The "conflict" implies that there is no single solution at the same time which can fulfill all objectives, yet a solution set. These solutions structure the Pareto-front in the objective space, and these solutions are called Pareto-optimal solutions and structure the Pareto Set in the decision space. Moreover, these solutions ought to equally distribute on the Pareto-front. To avoid this problem, a more convenient matrix number matrix is used.
- If the objective function includes conflicted terms, then we need to treat each objective function differently. But in our case, a single-objective problem based on judgment number is selected.
- The use of weights can be adapted as a single objective function for a multi-objective problem.
- In the multi-objective problem, the solution is not unique, and there is no unique, natural, and canonical solution concept.

C. CONSTRAINTS

1) POWER BALANCE OF MG

$$\sum_{i=1}^{N} P_i + P_{Grid} + P_{BS} = P_{Load} + P_{EVload} \tag{16}$$

where P_{Load}, P_{EVload}, P_{EVload}, and P_{BS} are load; EV power; and BSS output respectively.

2) POWER LIMITS

DGs power limits are expressed as:

$$P_{i\min} \le P_i \le P_{i\max} \tag{17}$$

where $P_{i\min}$ and $P_{i\max}$ are the minimum and maximum limit [29].

In the constraints of formulas (17), the limit of reactive power and voltage is not considered. As the EV load is active, we only considered active power, P. In ED problems, only limits of active power (P) are considered. Further, we do not measure voltage because it is not the load flow problem. Also, the DE ramp rate is considered as 1 kW/min, which is taken from the base paper. Because the voltage limit is directly related to power quality and power system security, further discussion and analysis about the voltage limit will be considered in the subsequent paper involving power flow analysis.

3) RAMP RATE LIMITS

DEs ramp rate is expressed as:

$$|P_G(t) - P_G(t-1)| \le r_{\max} * \Delta t \tag{18}$$

where $P_G(t)P_G(t-1)r_{\max}$ and t are outputs, maximum ramp rate, and time interval, respectively.

Regarding the ramp rates of different generators, the data is limited in research papers understandably, due to the confidential bidding of various market players, often data in research papers may not be a real picture. Formula 18 shows a ramp rate for the DEs, which is taken from the base paper. Future work will further include the different ramp rates of various generators. All factors will be considered comprehensively in the theoretical part.

4) BATTERY SOC

BSS of EVs in terms of SOC is expressed as:

$$SOC_{EV\,\min} \le SOC_{EV}(t) \le SOC_{EV\,\max} \tag{19}$$

where $SOC_{EV\,\min}$ and $SOC_{EV\,\max}$ are the minimum and maximum value of SOC [29]

5) LINE TRANSMISSION CAPACITY

Power flow between MG and PG is expressed as:

$$-P_{L\,\max} \le P_{Grid} \le P_{L\,\max} \tag{20}$$

where $P_{L\,\max}$ is the maximum capacity.

6) BATTERY OPERATION

Frequent charging and discharging of the battery will severely affect the lifetime. Following are the constraints which are expressed as follows:

$$SOC_{\min} \le SOC(t) \le SOC_{\max} \tag{21}$$

$$-P_{BS\,\max} \le P_{BS}(t) \le P_{BS\,\max} \tag{22}$$

$$SOC_{end} = SOC_{start} + \sum_{t=0}^{N-1} P_{BS}(t)\eta_C \Delta t = SOC_{start}$$

$$SOC_{end} = SOC_{start} + \sum_{t=0}^{N-1} \frac{P_{BS}(t)}{\eta_D} \Delta t = SOC_{start} \tag{23}$$

where $SOC_{\min}$ and $SOC_{\max}$ are the minimum and maximum SOC limits of the battery storage.$P_{BS\,\max}$, PBS(t) η_C, η_D are minimum and maximum value; maximum BSS power; charging and discharging efficiencies. SOC_{start} And SOC_{end} are the SOCs in the beginning and end of a cycle, respectively. Taking into account that the dynamic ED strategy for the MG is performed in cycles, an assumption may be applied that the battery SOC is equal between the beginning and the end of a cycle, as shown in formula (23).

IV. ECONOMIC DISPATCH STRATEGIES

Due to clean and renewable energy from PV and wind, the maximum utilization of PV-wind is ensured in this study. Different scheduling strategies for both operating modes of the MG are as follows:

A. GRID-CONNECTED OPERATION

The following two approaches of the scheduling strategies for economic MG operation are adopted in grid-connected mode.

1) SCHEDULING SCHEME 1

Electric vehicles are charging in autonomous mode. The load, which includes conventional and EV charging, is supplied by DGs and the PG. Power flow is in both directions.

2) SCHEDULING SCHEME 2

Electric vehicles are charging and discharging in coordinated mode. During the off-peak electricity pricing hours, EVs can be charged to store energy in EV batteries for discharging them at the peak pricing hours. The load, which includes conventional and EV charging, is supplied by renewables and PG. EVs start to discharge during peak pricing hours to feed the peak load, and DGs, PG, and EVs supply the system load. EVs are further used for transportation during parity hours, and DGs and PG supply the system load which includes only the conventional. Power flow is in both directions.

B. ISLAND OPERATION

The following two approaches of the scheduling strategies for economic MG operation are adopted in island mode.

1) SCHEDULING SCHEME 3

EVs are charging in autonomous mode. The system load, which is a combination of conventional and EV charging, is supplied by DGs. To avoid frequent charging and to discharge which will severely affect BSS life, BSS is used within a set time duration, i.e., off-peak hours from 23:00-24:00, 0:00-6:00, while peak hours from 17:00-23:00. When DGs output is not enough to meet the requirement, one portion will be shut off.

2) SCHEDULING SCHEME 4

EVs are charging and discharging in coordinated mode. The peak and off-peak load hours will be changed, which includes peak hours and off-peak hours. BSS is discharged 0:00-6:00 while it is charged at 17:00-24:00. The system load comprising of conventional and EV charging is supplied by distributed generators (DGS) and electric vehicles (EVs). When DGs output is not enough to meet the requirement, one portion will be shut off.

V. PSO ALGORITHM

A. PSO CONCEPT

PSO is a search and intelligence-based optimization, which is suggested by Kennedy and Eberhart in 1995 [29]. The main idea is to establish a swarming group with random numbers [33]. The position of every swarm can be represented as $X_i = (x_{i1}, x_{i2}, \ldots, x_{id})^T$, and while the velocity of every swarm is $V_i = (v_{i1}, v_{i2}, \ldots, v_{id})^T$, where $i = 1, 2, \ldots, n$, n is the population size. Every swarm continuously adjusts its position and velocity based on the expression shown below, until the termination criterion is reached:

$$\begin{cases} x_{i,d}^{k+1} = x_{i,d}^{k} + v_{i,d}^{k} \\ v_{i,d}^{k} = \omega v_{i,d}^{k} + c_1.rand_1^k. \\ \left(pbest_{i,d}^{k} - x_{i,d}^{k}\right) + c_2.rand_2^k.\left(gbest_{d}^{k} - x_{i,d}^{k}\right) \end{cases} \tag{24}$$

where $x_{i,d}^k$, $v_{i,d}^k$, ω, c_2, c_1, $pbest_{i,d}^k$, $gbest_d^k$, $rand_1^k$, and $rand_2^k$ are the position of a swarm i in k-th iteration; velocity; inertia weight factor; acceleration coefficients; personal best; global best; and random numbers respectively.

1) PSO PROCESS

- Step 1: Start initialization of swarm with its velocity and position, coefficients, and maximum iterations.
- Step 2: Set the objective as a fitness value.
- Step 3: Calculate the fitness for every swarm for personal best, while comparing with other swarms for global best.
- Step 4: Modify swarm velocity and position based on Equation (24).
- Step 5: Modify the personal best and global best solutions accordingly.
- Step 6: Repetitions of steps 4 and 5 until achieving the limit for maximum iterations.
- Step 7: The end product is global best, personal best, and its relevant position.

VI. ABC ALGORITHM

A. BASIC ABC CONCEPT

In 2005, Karaboga [18] had described a bee swarm algorithm called an artificial bee colony (ABC) algorithm for optimizing multi-variable numerical functions. The main idea is the intelligence and behavior of honey bee movements [34]. Using a global search algorithm like the ABC algorithm is the best method to combat the local extremes issues [34]. There are three players in bee colony foodstuffs: i) the food sources, ii) the employed bees, and iii) the unemployed bees, which are divided into onlooker and scout bees [34]. Employed bee examines a food source and executes a negotiation dancing after returning to a colony to attract visitors to its food supply. As the length of the dancing is related to the consistency of the food supply, stronger suppliers (global optima) have a higher chance that the onlooker bees should prefer. Once a food supply is depleted, the used bee is turned into a guide bee that looks unexpectedly for a fresh supply of food. This is a crucial stage in the feeding cycle as it helps prospective food suppliers to be found at minimal cost to the colony [35] and [18].

In the current study, the objective is to optimize the ED considering OC, PTC, and CE. The on-looker bee supervises and sends many employed bees to find the food source (i.e., the optimal size of DGs). While the scout bee brings the same solution during each specified iterations. The on-looker bee then checks the fitness (i.e., cost function) for the best solution and saves it in memory. During each iteration, an on-looker bee selects the best optimal solution out of multiple solutions after a specified number of iterations. In the second

phase, the scout bee is instructed by an on-looker bee to find the random food source (i.e., random solutions for DG size). For a global optimum solution, on-looker bee assigns the duty to the scout bee for a random search to avoid the trap in local minima. Therefore, ABC is a diversified algorithm that finds the global best optimal solution without trapping in the local minima, which shows its superior behavior, among other algorithms.

B. INITIAL SOLUTIONS

The initial factors in the ABC algorithm are the number of food points (NFP), which is equal to the total bees. The initial population for solutions is created by random numbers, with the following relationship for random positions [18]:

$$X_{ij} = X_{j,\min} + rand \times \left(X_{j,\max} - X_{j,\min}\right), \quad i = 1, 2, \ldots NFP,\ j = 1, 2, \ldots, J \tag{25}$$

where X_{ij} is the ith population of the jth vector and NFP is set to equal 5. $X_{j,\min}$ and $X_{j,\max}$ show the minimum and maximum boundaries of the jth vector. At the same time, rand is a random number that is uniformly distributed, ranging from 0 to 1. The following relationship can represent the fitness function:

$$Fitness_i = Obj\left(X_{ij}\right) + \sum_{m=1}^{M} \lambda_{eq,m} \left|h\left(X_{ij}\right)\right|^2 + \sum_{n=1}^{N} \lambda_{ineq,n} \left|g\left(X_{ij}\right) - g_{\lim}\right|^2 \tag{26}$$

where Obj is the objective function, while equality and inequality constraints are represented by $h\left(X_{ij}\right)$ and $g\left(X_{ij}\right)$ respectively. The penalty factors are abbreviated $\lambda_{eq,m}$ and $\lambda_{ineq,n}$ can be adjusted in the optimization process. $g_{\lim}$ can be defined as follows:

$$g_{\lim} = \begin{cases} X_j, & if\ X_{j,\min} \le X_j \le X_{j,\max} \\ X_{j,\min}, & if\ X_j < X_{j,\min} \\ X_{j,\max}, & if\ X_j > X_{j,\max} \end{cases} \tag{27}$$

The value of the penalty factor can be increased if one or more variables violate the limits, and the corresponding individual will, therefore, be discarded to skip the infeasible solution. The flowchart of the ABC algorithm is illustrated in Fig. 2.

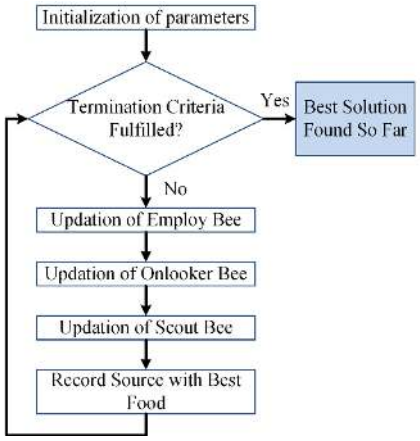

FIGURE 2. ABC optimization technique flowchart.

TABLE 3. EV parameters.

Parameter	Value
W100	13.90 kWh/100 km
CEV	21.60 kWh
$SOC(\max)$ & $SOC(\min)$	100% & 10%
P_C / P_{disC} (kW)	2.0–3.0
η	75.0 %

TABLE 4. DGs parameters.

DG Type	K_{Fuel} (PKR/kWh)	K_{OM} (PKR/kWh)	Incost (10^4 PKR/kW)	l (year)
Photovoltaic	-	0.0096	4.650	20.0
Wind	-	0.02960	2.375	20.0
Fuel Cell	0.2060	0.02930	4.275	10.0
Diesel Engine	0.3960	0.0880	1.600	10.0

TABLE 5. Emissions parameters.

type		CO_2	SO_2	NO_x
Processing cost (PKR/kg)		0.210	14.840	62.960
Emission Parameter weight (g/kWh)	Photovoltaic	0	0	0
	Wind	0	0	0
	Fuel Cell	489	0.003	0.01
	Diesel Engine	649	0.206	9.89
	Power Grid	889	1.8	1.6

VII. STUDY SYSTEM

This paper suggested an MG, including wind, solar, diesel engine, fuel cell, BSS and electric vehicles. In the grid-connected mode, the BSS is not active for scheduling due to the support from the power grid. In the islanded model, the BSS is actively participating in scheduling. There are 30 wind generators and 30 solar generators. The maximum capacity of wind and solar is 30 kW each. DEs and FCs are 60 kW each. DE ramp rate is 1 kW/min. BSS power is 150 kWh, with a power limit of 30 kW. The minimum and maximum value of SOC for BSS is 10% and 100%, respectively which is also mentioned in Table 3. The maximum line capacity is 300 kW. Energy buying and selling prices are real-time values for this paper. The compensation cost for the interrupted load (LS) is 1.450 PKR/kWh, and Table 3 shows EV parameters [29], and Table 4 shows DG parameters [29]. DGs means wind, solar, diesel and fuel cells. Table 5 shows the emissions coefficients and treatment costs [29]. Fig. 4 shows. Wind and solar power, load profile and real electricity price [29]. Different types of EVs are considered in this research. The number of EVs ranges from a minimum value of 80 to a maximum value of 700. Regarding

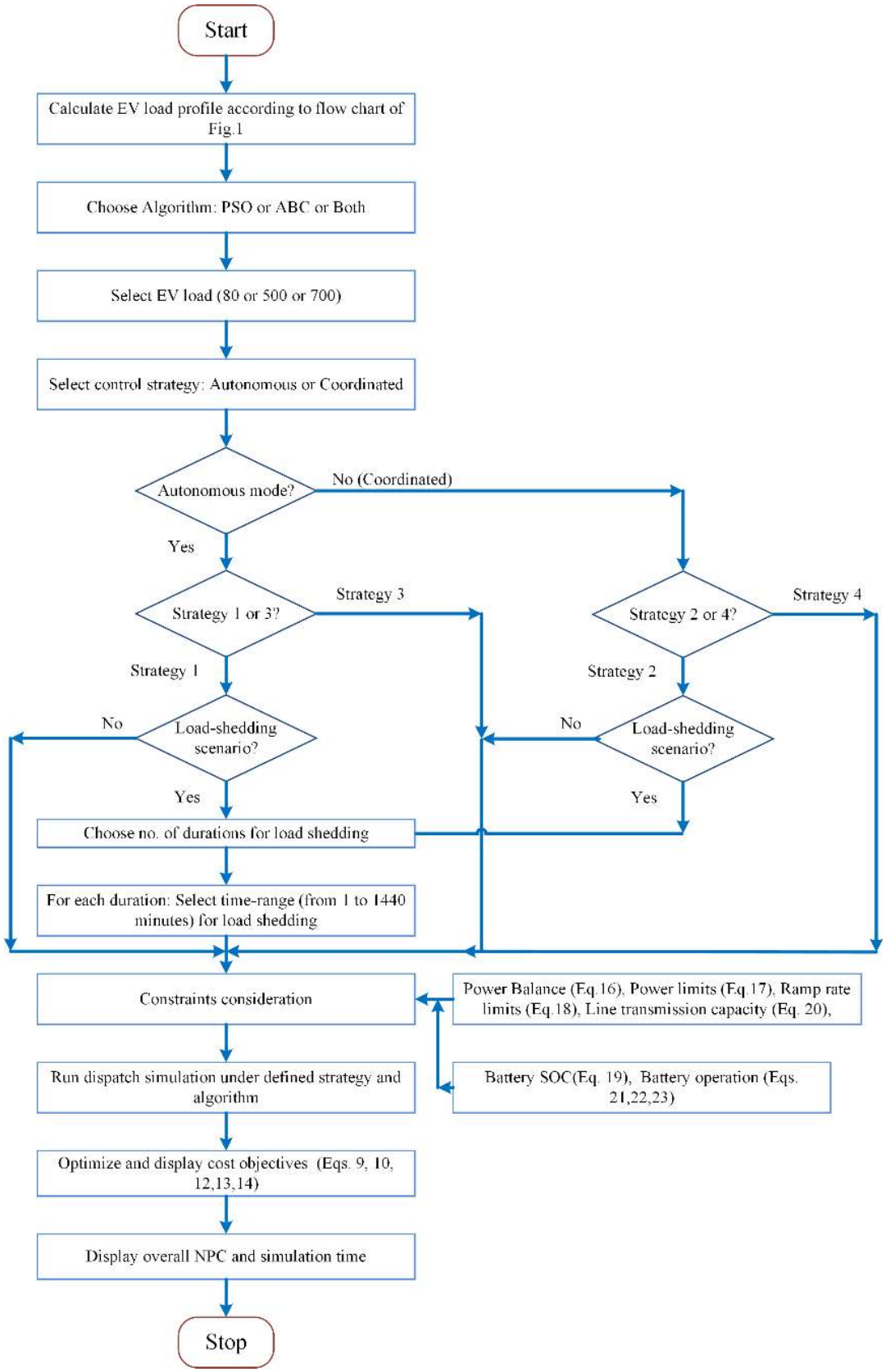

FIGURE 3. Flow chart of the employed ABC and PSO optimization methodologies.

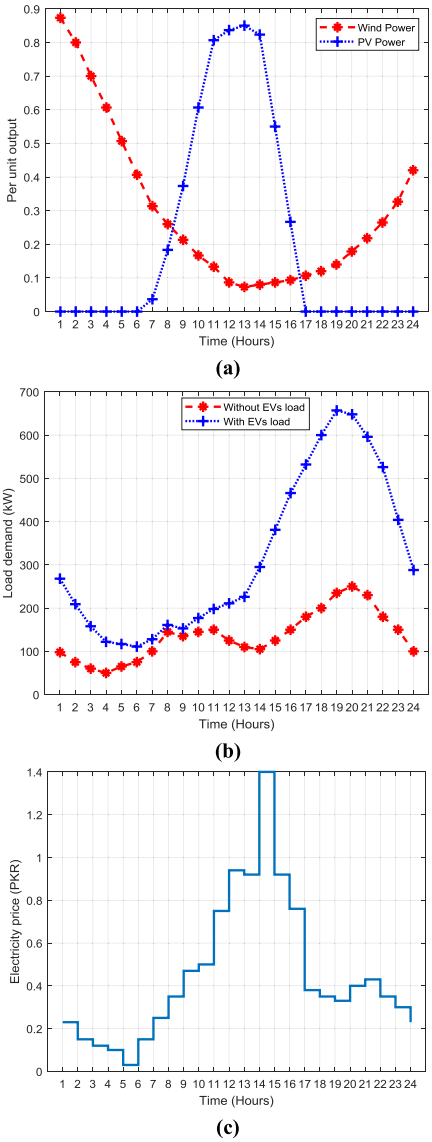

FIGURE 4. (a) The power output (wind & solar); (b) Load profile of MG; (c) Electricity rate.

the specific network topology of the MG, authors have used the parameters of the base paper by keeping the same MG topology, as mentioned in the base paper. The base of the real-time price set in Fig. 4(c) is taken from an article [29] which is already mentioned in the manuscript. Fig. 3 shows the flowchart of the proposed ABC and PSO optimization methodology.

The current study suggests a dispatch cycle of 1 day, which is subdivided into minute steps. The population size is 5, maximum iterations are 5, and the upper bound of the acceleration coefficient is set as 1.

A. SIMULATION ANALYSIS

Fig. 5 shows the simulation analysis of the everyday load of electric vehicles in various modes. Fig. 5a shows that the higher peak load is observed during more penetration of EVs.

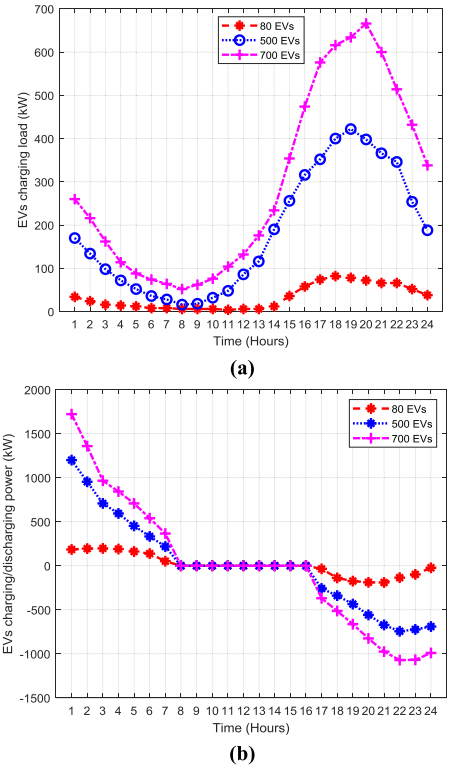

FIGURE 5. Load profile (a) autonomous mode; (b) coordinated mode.

The EV charging is analyzed at 18:00-19:00, which is a busy time, as vehicle owners usually start charging. The simulation analysis is precisely according to the priority of vehicle owners. If a large number of vehicles are charging suddenly, it will ultimately boost the burden on the utility grid. Fig. 5b elaborates vehicle charging at off-peak hours 0:00-8:00. This is consistent with MG stability, as well as economical due to the lowest electricity price. From 8:00 to 16:00, vehicles are used for transportation. Vehicles are discharging at 16:00-24:00 to contribute to ED.

B. COMPARISON BETWEEN PSO AND ABC

Scheduling strategy-1 is chosen to be the study case to investigate the performance of PSO and ABC algorithms. Fig. 6 shows the convergence value of fitness function, while Table 5 depicts parameters of PSO and proposed ABC algorithms. To find how scalable the proposed approach is, the comparison of fitness value for both algorithms (i.e., ABC and PSO) in Fig. 6 shows the fast convergence during the ABC method. Furthermore, the comparison Tables 5 also indicates the computational burden which is half in the case of the ABC method. For the computational cost of the proposed approach, Table 5 shows the simulation time of 4.098 s which is half as compared to that of PSO. Further, the computational cost is 395.01 PKR which is 2.23 % lower as compared to the PSO method. The fitness function which decides the computational burden is also shown in Figure 5 which shows fast convergence of the ABC convergence curve.

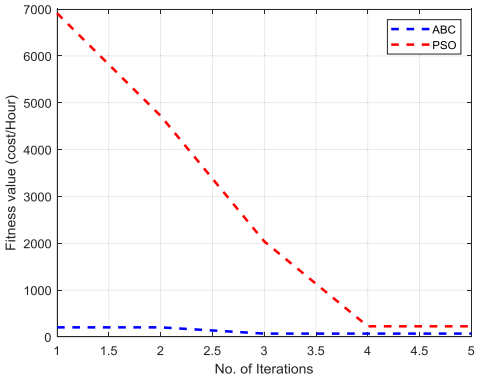

FIGURE 6. Convergence value for PSO and ABC.

Since ABC optimization is a heuristic search method, its optimization results have certain randomness. In all research studies, the convergence curve. normally decides the selection of the most suitable solution as the authors checked PSO and ABC algorithms while all heuristic algorithms do in the same way. Hence Fig 6 shows the effectiveness of the ABC algorithm over PSO. To further select the final solution, the authors took an average of twenty (20) optimization results, while an average of five (5) and even three (3) results were also enough in some cases where the variation trend of random numbers was negligible.

Fig. 6 elaborates that the ABC converges faster as compared to PSO. As depicted in Table 6, the total simulation time is also less for ABC. Based on the comparison of the convergence values of Table 6, it is verified that the proposed ABC is superior in performance as compared to PSO.

TABLE 6. Comparative analysis of the computational burden between two algorithms.

Algorithm	Simulation time/s	Convergence /PKR
PSO	8.932	404.03
ABC	4.098	395.01

C. SCHEDULING ANALYSIS IN THE GRID-CONNECTED MODE

1) DGS OUTPUT

After the ED of the MG, the outcome of the scheduling strategies of EVs, FCs, DEs, and PG are shown in Fig. 7. Due to the penetration maximization of renewables, the figures are not drawn with WT and PV.

During the scheduling strategy-1 of the MG system, Fig. 7a shows that the power grid output is negative from 0:00 to 5:30; i.e., the MG supplies extra energy to PG. the reason is that the WT output power is higher than the requirements of the MG. After 5:30, the renewables are ineffective in fulfilling the requirements; therefore, PG is used due to its lowest overall cost. Throughout the simulation period, FC is ON and is prioritized for scheduling due to a lower price. From 08:30 to 11:00, the cost of PG is more than FC; therefore, FC is added with PG to feed requirements.

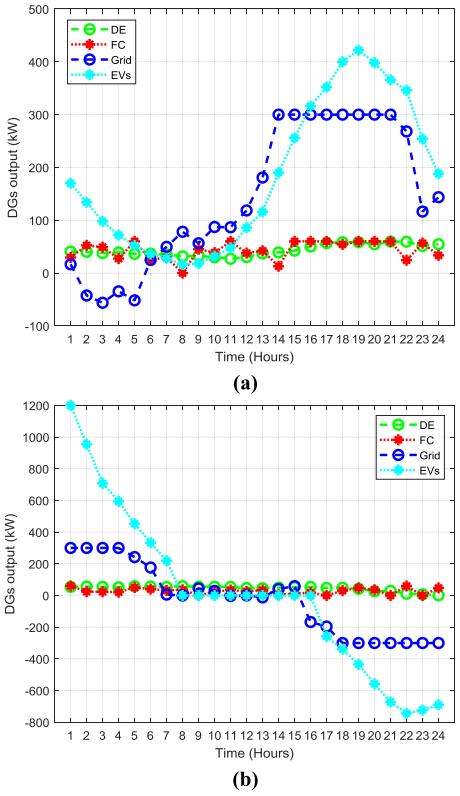

FIGURE 7. Economic dispatch (a) scheduling scheme 1; (b) scheduling scheme 2.

From 11:00 to 24:00, DE and FC have higher prices than PG, so PG for better economics supplies load demand.

When the scheduling strategy 2 of M is adopted, Fig. 7b shows that the vehicle's load is supplied at 0:00-8:00. Overall costs of PG and DE are lower than FC, therefore both provide energy with less power contribution from FC. Between 02:00-04:00 and 06:00-08:00, DE has a lower cost. During the interval starting from 8:00 to 16:00, vehicles are not active for scheduling. Before 13:00, the cost of DE is low as compared to FC and power grid, so it supplies more energy with FC and power grid. During interval 13:00-16:00, cost of the power grid and DE is low as compared to FC, therefore both supplies more energy with FC.

Meanwhile, when the costs of DE and FC are low as compared to PG (see Fig. 7b from 10:00-13:00), then extra power is supplied to PG for economical operation. After 16:00, the cost of DE and FC is low as compared to PG; therefore, the power grid is not used during this period. After 16:00, vehicles started to discharge and to contribute to scheduling; therefore, PG power is decreased, and vehicles began to supply energy to PG for the economical operation.

2) COST FUNCTION

Table 7 shows the cost for individual functions as well as an overall comprehensive single objective for both strategies. Table 7 depicts average values after repeatedly computing ten times.

TABLE 7. Grid-connected scheme: dispatch results (pkr) under scheduling schemes 1 and 2.

Algorithm	Cost objective	Scheduling **scheme** 1	Scheduling **scheme** 2	Change (%Δ)
PSO	C1	4353.9879	3588.0823	-17.59
	C2	788.2612	553.207	-29.82
	C3	404.0335	302.3373	-25.17
	C	3019.4004	2460.1565	-18.52
ABC	C1	4260.6187	3503.9052	-17.76
	C2	884.1023	620.243	-29.84
	C3	395.0063	294.1912	-25.52
	C	2983.7349	2422.9982	-18.79

From the values of Table 7, it is observed that selecting scheduling strategy 2 with ABC algorithm decreases the cost by 18.79%, which is the single objective cost as compared to the selection of strategy 1. Further, it reduces 17.76% of the operating cost, 29.84% pollutant emissions, and 25.52% the carbon dioxide emissions. While simulation studies with the same strategies are also carried out by using the PSO algorithm, it is observed that selecting scheduling strategy 2 with the PSO algorithm decreases the cost by 18.52%, which is the single objective cost as compared to the selection of strategy 1. Further, it reduces 17.59% of the operating cost, 29.82% pollutant emissions, and 25.17% the carbon dioxide emissions. The simulation study elaborates that vehicle coordinated mode can reduce all three objectives costs during the grid-connected mode of the MG. This is also verified that the best results are found with the proposed ABC algorithm, as shown in Table 7.

Different results obtained in Table 8 are analyzed that all the objectives are achieved with their best costs by opting proposed ABC algorithm as compared to the PSO algorithm. This concludes the observation shown in Table 8 that ABC is showing slightly better performance as compared to the PSO algorithm to minimize the comprehensive cost (1.46%), operating cost (0.97%), carbon emission cost (0.07%), and pollutant treatment cost which is 1.39%.

TABLE 8. Comparison (pkr) of PSO and ABC under scheduling strategies 1 and 2.

Cost objective	PSO	ABC	Improvement (%)
C1	-17.59	-17.76	0.97
C2	-29.82	-29.84	0.07
C3	-25.17	-25.52	1.39
C	-18.52	-18.79	1.46

Based on Fig. 8a and Fig. 8b, vehicles are charging during off-peak hours, and discharging during peak hours to accomplish the target of peaks shifting as well as to lower the cost of buying energy units from PG. Therefore, vehicles are efficient in coordinated mode and are contributing to MG stability as well as cost reduction.

D. SCHEDULING ANALYSIS IN THE ISLAND MODE

1) DGS OUTPUT

After the ED of the MG, the outcome of the scheduling strategies of EVs, FCs, DEs, and PG are shown in Fig. 6.

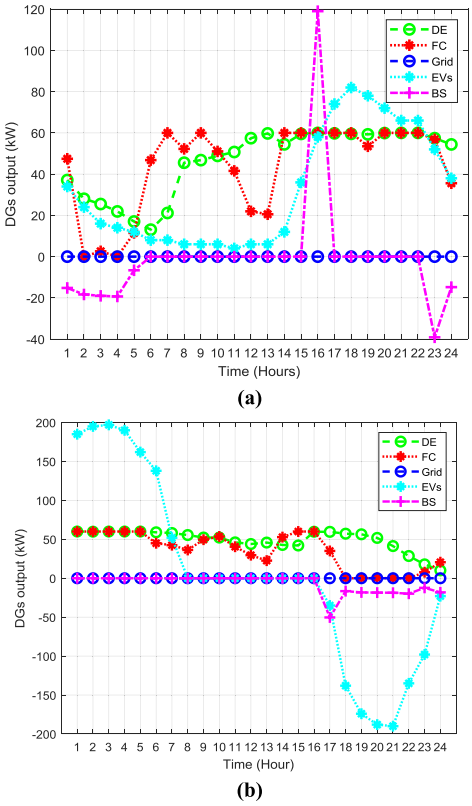

FIGURE 8. Dispatch results (a) scheduling scheme 3; (b) scheduling scheme 4.

Due to the penetration maximization of renewables, the figures are not drawn with WT and PV.

When scheduling strategy 3 of the MG system is adopted, Fig. 8a shows that the BSS is charging during the period 0:00-6:00, because the MG load is less, and DE and FC supply power afterward. From 12:00 to 13:00, FC is unable to meet the demand, and BSS is not in service so far, while power shortfall is observed, therefore part of the load needs to be shut off. During the time interval, 15:00-16:00. EVs are connected for charging, and the BSS feeds the excess power. During 16:00-22:00, more shortage is observed due to vehicle charging, and meanwhile, BSS starts to discharge energy for low peak and low power shortage. After 22:00, MG demand is reduced and wind, solar, DE, and FC are fulfilling the load requirements as well as charging of the BSS.

During MG operation with scheduling strategy 4, Fig. 8b shows that vehicle charging occurred at 0:00-8:00, which drastically increases the power demand while DE and FC powers are sufficient to fulfill this requirement, so the BSS is controlled to remain in idle state. Time duration at 8:00-16:00 is not involved in vehicle scheduling, and the power demand is supplied by both DE and FC. DE and FC power is unable to fulfill load requirements at 16:00-17:00, and the BSS supplies the power mismatch. After 16:00, vehicles start discharging to contribute to scheduling while charging the BSS at the same time. Further, the FC is not participating from 18:00 to 22:00 due to the high participating

cost. After 18:00, DE and FC power-sharing are gradually decreasing due to their higher price as compared to that of V2G until FC is not involved in delivering power at 18:00 while DE reduces its output from 20:00 onwards.

2) COST FUNCTION

Table 9 shows the cost for individual functions as well as an overall comprehensive single objective for both strategies. Table 9 depicts average values after repeatedly computing 10 times.

TABLE 9. Island Operation: dispatch results (pkr) under scheduling schemes 3 and 4.

Algorithm	Cost objective	Scheduling **scheme** 3	Scheduling **scheme** 4	Change (%Δ)
PSO	C1	4074.1311	3266.451	-19.82
	C2	830.1231	800.3004	-3.59
	C3	320.678	260.0912	-18.89
	C	2843.2173	2314.6784	-18.59
ABC	C1	4094.5036	3048.4961	-25.55
	C2	886.5526	705.8325	-20.38
	C3	328.4179	234.1	-28.72
	C	2871.5807	2148.7188	-25.17

The data of Table 9 shows improvement results after adopting the scheduling strategy 4. ABC algorithm reduces the overall single objective cost by 25.17% as compared with taking the scheduling strategy 3. Further, the scheduling strategy 4 reduces the operating cost by 25.55%, reduces the pollutant emissions by 20.38%, and reduces the carbon dioxide emissions by 28.72%. When the PSO algorithm is applied with the same strategies, it is observed that it reduces the overall single objective cost by 18.59% as compared with adopting the scheduling strategy 3. Further, the scheduling strategy 4 reduces the operating cost by 19.82%, reduces the pollutant emissions by 3.59%, and reduces the carbon dioxide emissions by 18.89%. This verifies the superior performance of the proposed methodology with ABC that the vehicle coordination for charging and discharging mode is reducing the operating cost, pollutant emissions, and the carbon dioxide emissions while MG is running under the standalone (islanded) mode. Vehicles charging enhances peak loads while following the vehicles (EVs) charging in autonomous mode, leading to a substantial recompense cost due to the loss of interruptible loads (LOIL), as shown in Fig. 6a. At the same time, the vehicles operating in discharging mode obviates a significant part of LOIL while pursuing the vehicles charging and discharging in coordination mode (see Fig. 6b), hence it reduces the operating cost, pollutant emissions, and the carbon dioxide emissions. By concluding the remarks of this section, the selection of the vehicle's coordination in charging and discharging mode will surely trim the demand shortage during the MG operation in standalone mode, which will assist in getting a better operation in terms of economics.

Different results obtained in Table 10 are analyzed that all the objectives are achieved with their best costs by opting proposed ABC algorithm as compared to the PSO algorithm. This concludes the observation shown in Table 12 that ABC is showing significantly better performance to minimize the comprehensive cost (35.40%), operating cost (28.91%), and carbon emission cost (52.04%). In comparison, drastically significant improvement with ABC algorithm is observed in reducing pollutant treatment cost which is 467.69%.

TABLE 10. Comparison (pkr) of pso and abc under scheduling strategies 3 and 4.

Cost objective	PSO	ABC	Improvement (%)
C1	-19.82	-25.55	28.91
C2	-3.59	-20.38	467.69
C3	-18.89	-28.72	52.04
C	-18.59	-25.17	35.40

E. SCHEDULING ANALYSIS WITH CONSIDERATION OF LOAD SHEDDING IN THE GRID-CONNECTED MODE

1) DGS OUTPUT

After the ED of the MG, the outcome of the scheduling strategies of EVs, FCs, DEs, and PG are shown in Fig. 9. Due to the penetration maximization of renewables, the figures are not drawn with WT and PV.

During the scheduling strategy 1 of the MG system, forced load shedding is carried out from 01:40 to 02:20, as shown in Fig. 9(a1). However, the power grid output is positive throughout the simulation time; i.e., the power grid supplies excess electricity to the MG. This is because the PV output power is zero, while wind power is insufficient to feed the load requirements. So, the power grid is used due to its lowest overall objective cost. Throughout the simulation period, DE is enabled and is prioritized to be scheduled due to its lower objective cost. From 14:00 to 22:00, the cost of PG turns lowest among all DGs, so the power grid feeds most of the power demand. From 07:00 to 24:00, DE and FC costs are higher than that of PG; hence most of the load demand is supplied by PG for improvement of the economics.

Similarly, Fig. 9(a2) shows the DGs output power during load shedding from 10:00 to 11:40, while Fig. 9(a3) shows the DGs power when load shedding is executed from 16:40 to 20:00.

When the scheduling strategy 2 of MG is adopted, forced load shedding is carried out from 01:40 to 02:20, which is shown in Fig. 9(b1). Fig. 9(b1) depicts the vehicle charging load at 0:00-8:00, while overall PG cost is lower than FC and DE, so the power grid provides output power together with less power contribution from FC and DE. From 8:00 to 16:00, vehicles are not participating in scheduling, while 16:00-19:00 time range shows lower DE cost as compared to the FC; therefore, it supplies power. After 16:00, vehicles follow the discharging mode, and contributing in the scheduling; therefore PG power is decreased, and vehicles started to provide output to PG, and the economic benefits for vehicle owners are ensured.

Similarly, Fig. 9(b2) shows the DGs output power during load shedding from 10:00 to 11:40, while Fig. 9(b3) shows the DGs power when load shedding is executed from 16:40 to 20:00.

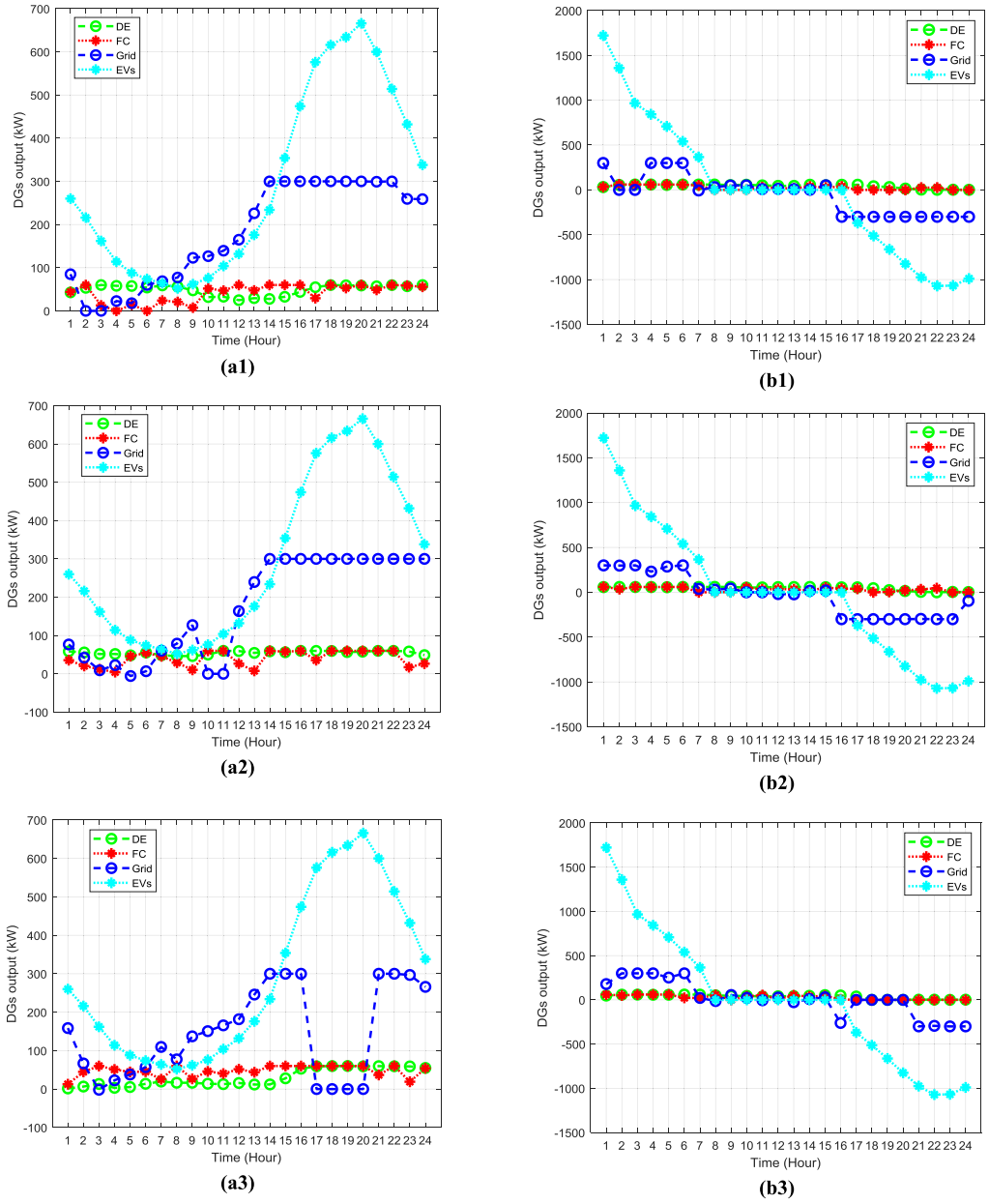

FIGURE 9. Dispatch results with load shedding scenarios 1-3 (a) scheduling scheme 1; (b) scheduling scheme 2.

To verify the work and to validate the presented method sufficiently, the authors run multiple simulation results. Table 6-9 shows the average values of twenty (20) simulation results, while one solution set in the form of Figures 6-8 is selected, and almost the same DGs trend was observed in these results. Hence, more results were only skipped for the reader to avoid any repetition with more number of pages.

2) COST FUNCTION

Table 11 shows the cost for individual functions as well as an overall comprehensive single objective for both strategies. Table 11 depicts average values after repeatedly computing two times.

It is observed from Table 11 that by selecting scheduling strategy, 2 for LSS-1 with PSO reduces by 78.29% the comprehensive single objective cost as compared to the selection of scheduling strategy 1. While strategy-2 also reduces by 79.25% the operating cost, reduces by 57.04% pollutant emissions, and decreases by 90.72% the carbon dioxide emissions. Results for scheduling strategy 2 for LSS-2 and LSS-3 with PSO are also shown in Table 11. It is also observed from Table 11 that by selecting scheduling strategy, 2 for LSS-1 with ABC reduces by 79.57% the comprehensive single objective cost as compared to the selection of scheduling strategy 1. While strategy-2 also reduces by 80.55% the operating cost, reduces by 58.59% pollutant emissions, and decreases by 92.23% the carbon dioxide emissions.

TABLE 11. Grid-connected Operation: dispatch results (pkr) under scheduling schemes 1 and 2.

Algorithm	load shedding scenario	Cost/PKR	Scheduling scheme 1	Scheduling scheme 2	Change (%Δ)
PSO	1	C1	9431.4374	1956.6255	-79.25
		C2	1304.4164	560.3748	-57.04
		C3	1041.0994	96.5981	-90.72
		C	6453.7595	1401.2291	-78.29
	2	C1	9171.9965	2710.3495	-70.45
		C2	1329.7963	701.8563	-47.22
		C3	1011.1615	194.5498	-80.76
		C	6291.9167	1928.1515	-69.36
	3	C1	8043.2585	3724.1134	-53.70
		C2	1125.6114	538.5386	-52.16
		C3	862.6207	323.6689	-62.48
		C	5504.6175	2545.2529	-53.76
ABC	1	C1	9418.3993	1831.9149	-80.55
		C2	1332.349	551.7836	-58.59
		C3	1037.0017	80.5783	-92.23
		C	6452.2402	1317.8921	-79.57
	2	C1	9337.0119	2594.7108	-72.21
		C2	1207.0991	620.3497	-48.61
		C3	1020.3584	176.4603	-82.71
		C	6366.3018	1831.5425	-71.23
	3	C1	8134.5249	3901.9083	-52.03
		C2	994.7689	682.8468	-31.36
		C3	866.0267	348.2228	-59.79
		C	5529.3141	2698.3538	-51.20

Results for scheduling strategy 2 for LSS-2 and LSS-3 with ABC are also shown in Table 11. This simulation result elaborates that the vehicle's coordination in charging and discharging mode is reducing the operating cost, carbon emissions and pollutant emissions during the grid-connected mode of the MG. This is also verified that all the objectives are achieved with their best prices by opting proposed ABC algorithm as compared to the PSO algorithm. Contradictory performance between PSO and ABC is observed only in one case i.e., LSS-3, when PSO beats ABC in cost minimization of three objectives. In this case, PSO reduces by 53.76% the comprehensive single objective cost as compared to the selection of scheduling strategy 1. While strategy-2 also reduces by 53.70% of the operating cost, reduces by 52.16% pollutant emissions, and decreases by 62.48% of the carbon dioxide emissions.

On the other hand, ABC reduces by 51.20% the comprehensive single objective cost as compared to the selection of scheduling strategy 1. While strategy-2 also reduces by 52.03% the operating cost, reduces by 31.36% pollutant emissions, and decreases by 59.79% of the carbon dioxide emissions. Different results shown in Table 12 are analyzed that all the objectives are achieved with their best costs by opting for the PSO algorithm instead of the proposed ABC algorithm. This concludes the observation shown in Table 12 that PSO is showing slightly better performance during peak load hours to minimize the comprehensive cost (4.76%), operating cost (3.11%) and carbon emission cost (4.31%) while significant improvement with PSO is observed in reducing pollutant treatment cost which is 39.88%.

Based on Fig. 5a, and Fig. 5b, the vehicles are charging during off-peak hours and discharging during peak hours for peaks shifting and to lower the buying cost of energy

TABLE 12. Comparative analysis (pkr) of PSO and ABC under load shedding scenarios.

load shedding scenario	Cost objective	PSO	ABC	Improvement (%)
1	C1	-79.25	-80.55	1.64
	C2	-57.04	-58.59	2.72
	C3	-90.72	-92.23	1.66
	C	-78.29	-79.57	1.63
2	C1	-70.45	-72.21	2.50
	C2	-47.22	-48.61	2.94
	C3	-80.76	-82.71	2.41
	C	-69.36	-71.23	2.70
3	C1	-53.70	-52.03	-3.11
	C2	-52.16	-31.36	-39.88
	C3	-62.48	-59.79	-4.31
	C	-53.76	-51.20	-4.76

units from PG. Therefore, the vehicle's coordination in both (charging and discharging) mode under different LSSs contributes to the MG stability, as well as declines the comprehensive single objective cost, the operating cost, pollutant, and the carbon dioxide emissions. Similarly, LSS-2 during load shedding from 10:00 to 11:40 while LSS-3 during load shedding duration from 16:40 to 20:00 also shows a similar trend in reducing the overall single objective function cost as well as the operating cost, pollutant and the carbon dioxide emissions.

VIII. CONCLUSION

Keeping in view the natural (spatial and temporal) behaviors of vehicles, two vehicles (EVs) models are presented in this paper. By considering the current investigations on multi-objective ED of the MG to determine minimum possible values, three main and crucial daily life factors are considered as the objective functions. Five control and optimization

techniques for standalone and grid-connected modes of the MG operations are established. Further, V2G based multi-objective ED model of the MG system is developed, and the judgment matrix methodology is used to convert it into a single objective. Keeping in view the safety constraints, the model validity, along with the algorithms, is verified through simulation of the case studies by using PSO and ABC algorithms under different scheduling strategies. With the use of the ABC algorithm, the simulation studies depict the superior performance of vehicles with charging/discharging in a coordinated mode in terms of better operation economics as compared to the autonomous charging mode. Further, the dual-mode (seamless transition) is also analyzed during load shedding hours with consideration of three different scenarios. During LSS-3 with load shedding during peak hours, it is observed that PSO has slightly better performance to minimize the comprehensive cost, operating cost and carbon emission cost while significant improvement with PSO is observed in reducing pollutant treatment cost. This concludes the observation that ABC is better in V2G based MG with coordinated charging and discharging mode. At the same time, its performance is significant during a large number of EVs (i.e., 700 EVs instead of 80EVs) while PSO performed better with the case of load shedding during peak hours. The future work includes some EVs which don't obey the dispatching strategy proposed in this paper.

ACKNOWLEDGMENT

The authors like to express their sincere gratitude to the Renewable Energy research lab, College of Engineering, Prince Sultan University, Riyadh, Saudi Arabia, for providing technical support.

REFERENCES

[1] R. H. Lasseter and P. Piagi, "Microgrid: A conceptual solution," in *Proc. PESC*, Jun. 2004, pp. 4285–4290.
[2] S. Wang, L. Lu, X. Han, M. Ouyang, and X. Feng, "Virtual-battery based droop control and energy storage system size optimization of a DC microgrid for electric vehicle fast charging station," *Appl. Energy*, vol. 259, Feb. 2020, Art. no. 114146.
[3] R. C. Green, L. Wang, and M. Alam, "The impact of plug-in hybrid electric vehicles on distribution networks: A review and outlook," *Renew. Sustain. Energy Rev.*, vol. 15, no. 1, pp. 544–553, Jan. 2011.
[4] J. A. P. Lopes, F. J. Soares, and P. M. R. Almeida, "Integration of electric vehicles in the electric power system," *Proc. IEEE*, vol. 99, no. 1, pp. 168–183, Jan. 2011.
[5] W. Kempton and J. Tomić, "Vehicle-to-grid power fundamentals: Calculating capacity and net revenue," *J. Power Sources*, vol. 144, no. 1, pp. 268–279, Jun. 2005.
[6] R. Shi, S. Li, P. Zhang, and K. Y. Lee, "Integration of renewable energy sources and electric vehicles in V2G network with adjustable robust optimization," *Renew. Energy*, vol. 153, pp. 1067–1080, Jun. 2020.
[7] X. Li, Y. Tan, X. Liu, Q. Liao, B. Sun, G. Cao, C. Li, X. Yang, and Z. Wang, "A cost-benefit analysis of V2G electric vehicles supporting peak shaving in Shanghai," *Electric Power Syst. Res.*, vol. 179, May 2020, Art. no. 106058.
[8] M. Basu, "Dynamic economic emission dispatch using nondominated sorting genetic algorithm-II," *Int. J. Electr. Power Energy Syst.*, vol. 30, no. 2, pp. 140–149, Feb. 2008.
[9] X. Zhang, K. W. Chan, H. Wang, B. Zhou, G. Wang, and J. Qiu, "Multiple group search optimization based on decomposition for multi-objective dispatch with electric vehicle and wind power uncertainties," *Appl. Energy*, vol. 262, Mar. 2020, Art. no. 114507.
[10] L. T. Al-Bahrani, B. Horan, M. Seyedmahmoudian, and A. Stojcevski, "Dynamic economic emission dispatch with load demand management for the load demand of electric vehicles during crest shaving and valley filling in smart cities environment," *Energy*, vol. 195, Mar. 2020, Art. no. 116946.
[11] R. T. F. A. King and H. C. S. Rughooputh, "Elitist multiobjective evolutionary algorithm for environmental/economic dispatch," in *Proc. Congr. Evol. Comput.*, 2003, pp. 1108–1114.
[12] X. Shaoyu, W. Xiuli, Q. Chong, W. Xifan, and G. Jingli, "Impacts of different wind speed simulation methods on conditional reliability indices," *Int. Trans. Electr. Energy Syst.*, vol. 25, no. 2, pp. 359–373, Feb. 2015.
[13] M. Rajkumar, K. Mahadevan, S. Kannan, and S. Baskar, "NSGA-II technique for multi-objective generation dispatch of thermal generators with nonsmooth fuel cost functions," *J. Electr. Eng. Technol.*, vol. 9, no. 2, pp. 423–432, Mar. 2014.
[14] H. Hou, M. Xue, Y. Xu, Z. Xiao, X. Deng, T. Xu, P. Liu, and R. Cui, "Multi-objective economic dispatch of a microgrid considering electric vehicle and transferable load," *Appl. Energy*, vol. 262, Mar. 2020, Art. no. 114489.
[15] M. M. Esfahani and O. Mohammed, "Real-time distribution of en-route electric vehicles for optimal operation of unbalanced hybrid AC/DC microgrids," *eTransportation*, vol. 1, Aug. 2019, Art. no. 100007.
[16] Z. Wang, Y. Tang, X. Chen, X. Men, J. Cao, and H. Wang, "Optimized daily dispatching strategy of building-integrated energy systems considering vehicle to grid technology and room temperature control," *Energies*, vol. 11, no. 5, p. 1287, 2018.
[17] L. Polanco Vasquez, C. Carreño Meneses, A. Pizano Martínez, J. López Redondo, M. Pérez García, and J. Álvarez Hervás, "Optimal energy management within a microgrid: A comparative study," *Energies*, vol. 11, no. 8, p. 2167, 2018.
[18] W.-M. Lin, C.-S. Tu, and M.-T. Tsai, "Energy management strategy for microgrids by using enhanced bee colony optimization," *Energies*, vol. 9, no. 1, p. 5, 2015.
[19] J. Ben Hmida, M. Javad Morshed, J. Lee, and T. Chambers, "Hybrid imperialist competitive and grey wolf algorithm to solve multiobjective optimal power flow with wind and solar units," *Energies*, vol. 11, no. 11, p. 2891, 2018.
[20] D. Liu, Q. Zhong, Y. Wang, and G. Liu, "Modeling and control of a V2G charging station based on synchronverter technology," *CSEE J. Power Energy Syst.*, vol. 4, no. 3, pp. 326–338, Sep. 2018.
[21] S. Al-Sakkaf, M. Kassas, M. Khalid, and M. A. Abido, "An energy management system for residential autonomous DC microgrid using optimized fuzzy logic controller considering economic dispatch," *Energies*, 2019.
[22] U. Abronzini, C. Attaianese, M. D'Arpino, M. Di Monaco, and G. Tomasso, "Cost minimization energy control including battery aging for multi-source EV charging station," *Electronics*, vol. 8, no. 1, p. 31, 2019.
[23] Y. Li, X. Fan, Z. Cai, and B. Yu, "Optimal active power dispatching of microgrid and distribution network based on model predictive control," *Tsinghua Sci. Technol.*, vol. 23, no. 3, pp. 266–276, Jun. 2018.
[24] H. Hou, M. Xue, Y. Xu, J. Tang, G. Zhu, P. Liu, and T. Xu, "Multiobjective joint economic dispatching of a microgrid with multiple distributed generation," *Energies*, vol. 11, no. 12, p. 3264, 2018.
[25] G. Saldaña, J. I. San Martin, I. Zamora, F. J. Asensio, and O. Oñederra, "Electric vehicle into the grid: Charging methodologies aimed at providing ancillary services considering battery degradation," *Energies*, vol. 12, no. 12, p. 2443, 2019.
[26] L. Yu, T. Zhao, Q. Chen, and J. Zhang, "Centralized bi-level spatial-temporal coordination charging strategy for area electric vehicles," *CSEE J. Power Energy Syst.*, vol. 1, no. 4, pp. 74–83, Dec. 2015.
[27] D. Liu, Y. Wang, and Y. Shen, "Electric vehicle charging and discharging coordination on distribution network using multi-objective particle swarm optimization and fuzzy decision making," *Energies*, vol. 9, no. 3, p. 186, 2016.
[28] R. Shi, S. Li, C. Sun, and K. Lee, "Adjustable robust optimization algorithm for residential microgrid multi-dispatch strategy with consideration of wind power and electric vehicles," *Energies*, vol. 11, no. 8, p. 2050, 2018.
[29] H. Liu, Y. Ji, H. Zhuang, and H. Wu, "Multi-objective dynamic economic dispatch of microgrid systems including vehicle-to-grid," *Energies*, vol. 8, no. 5, pp. 4476–4495, 2015.
[30] D. Vyas and A. Santini. *Use of National Surveys for Estimating 'Full' PHEV Potential For Oil Use Reduction*. [Online]. Available: https://www.anl.gov/es

[31] Z.-S. Xu and J. Chen, "Approach to group decision making based on interval-valued intuitionistic judgment matrices," *Syst. Eng.-Theory Pract.*, vol. 27, no. 4, pp. 126–133, Apr. 2007.
[32] J. Kennedy, "Particle swarm optimization," in *Encyclopedia of Machine Learning and Data Mining*, C. Sammut and G. I. Webb, Eds. Boston, MA, USA: Springer, 2010, pp. 760–766.
[33] T. L. Saaty, "How to make a decision: The analytic hierarchy process," *Interfaces*, vol. 24, no. 6, pp. 19–43, Dec. 1994.
[34] D. Karaboga and B. Basturk, "A powerful and efficient algorithm for numerical function optimization: Artificial bee colony (ABC) algorithm," *J. Global Optim.*, vol. 39, no. 3, pp. 459–471, Oct. 2007.
[35] F. M. Janeiro, Y. Hu, and P. M. Ramos, "Peak factor optimization of multi-harmonic signals using artificial bee colony algorithm," *Measurement*, vol. 150, Jan. 2020, Art. no. 107040.

HABIB UR RAHMAN HABIB was born in Fort Abbas, Pakistan, in 1988. He received the B.Sc. degree in electrical engineering and the M.Sc. degree in electrical power engineering from the University of Engineering and Technology at Taxila, Pakistan, in 2009 and 2015, respectively. He is currently pursuing the Ph.D. degree with the State Key Laboratory of Advanced Electromagnetic Engineering and Technology, Huazhong University of Science and Technology, Wuhan, China. Since 2009, he has been with the COMSATS Institute of Information Technology, Pakistan, and the Wah Engineering College, University of Wah, Pakistan. He has been a Management Trainee Officer (Maintenance Department) with Dynamic Packaging Pvt., Ltd., Lahore, Pakistan. He is also permanently with the Department of Electrical Engineering, University of Engineering and Technology at Taxila. His research interests include electrical planning and estimation, energy resources and planning, modeling and simulation, renewable energy technology and management, smart grid applications in power systems, distributed generation and microgrid, power electronics, power quality, artificial intelligence, deep learning, fuzzy controllers, heuristic algorithms design and optimization, energy economics, and model predictive control and its application in the power industry.

UMASHANKAR SUBRAMANIAM (Senior Member, IEEE) is currently an Associate Professor with the Renewable Energy Laboratory, College of Engineering, Prince Sultan University, Saudi Arabia. He has more than 15 years of teaching, research, and industrial R&D experience. Previously, he worked as an Associate Professor and the Head of VIT, Vellore. He is a Senior R&D and a Senior Application Engineer in the field of power electronics, renewable energy, and electrical drives. He has published more than more than 250 research articles in national and international journals and conferences. He has also authored/coauthored/contributed 12 books/chapters and 12 technical articles on power electronics applications in renewable energy and allied areas. He is a Senior Member of PES, IAS, PSES, YP, and ISTE. He is also an Associate Editor of IEEE Access. He received the Danfoss Innovator Award-Mentor, from 2014 to 2015 and 2017 to 2018, the Research Award by VIT University, from 2013 to 2018, the INAE Summer Research Fellowship, in 2014. He has taken charge as the Vice-Chair of the IEEE Madras Section and the Chair of the IEEE Student Activities, from 2018 to 2020. He was an Executive Member, from 2014 to 2016, and the Vice-Chair of the IEEE MAS Young Professional by the IEEE Madras Section, from 2017 to 2019. He is an Editor of Heliyon, an Elsevier journal, and various other reputed journals. Under his guidance 24 PG students and more than 25 UG Students completed the senior design project work. Also six Ph.D. scholars completed Doctoral thesis as Research Associate. He is also involved in collaborative research projects with various international and national level organizations and research institutions.

ASAD WAQAR received the Electrical Engineering degree from UET Taxila, in 2002, the master's degree in electrical power engineering from RWTH Aachen, Germany, in 2011, and the Ph.D. degree in electrical engineering from the Huazhong University of Science and Technology, China, in 2016. He is currently working as an Associate Professor with the Department of Electrical Engineering, Bahria University, Islamabad, Pakistan. His research interests include smart grids, microgrids operation and control, power quality, power electronics, energy economics, and network reinforcement planning.

BASHAR SAKEEN FARHAN received the B.Sc. degree in electrical and electronic engineering from the College of Engineering, Al-Mustansiriya University, Iraq, in 2004, the M.Tech. degree in power system from SHIATS, India, in 2013, and the Ph.D. degree in electrical engineering from HUST, China, 2017. He was an Engineer to Bagdad Governorate–Bagdad Governorate Directorate of Water, Iraq, from 2005 to 2019. He joined the Electrical Engineering Department, Engineering College, Al-Iraqia University, in December 2019.

KOTB M. KOTB received the B.Sc. and M.Sc. degrees in electrical engineering from Tanta University, Egypt, in 2012 and 2017, respectively. He is currently pursuing the Ph.D. degree with the Budapest University of Technology and Economics, Budapest, Hungary. He started working as a Teaching Assistant at the Department of Electrical Power and Machines Engineering, Faculty of Engineering, Tanta University, in 2013, where he was promoted to the degree of Assistant Lecturer, in May 2017. His research interests include power electronics, renewable energy systems, and microgrid technologies.

SHAORONG WANG received the B.Sc. degree in electrical engineering from Zhejiang University, Hangzhou, China, in 1984, the M.Sc. degree in electrical engineering from North China Electric Power University, China, in 1990, and the Ph.D. degree from the Huazhong University of Science and Technology, China, in 2004. He is currently a Professor with the School of Electrical and Electronics Engineering, Huazhong University of Science and Technology. His research interests include power system operation and control, power grid planning, active distribution networks, AI and big data applications in power systems, and robotic inspection in power systems.